

The use of stable isotope-labeled glycerol and oleic acid to differentiate the hepatic functions of DGAT1 and -2

Jenson Qi,^{1,*} Wensheng Lang,^{*} John G. Geisler,^{*} Ping Wang,^{*} Ioanna Petrounia,[†] Selyna Mai,[†] Charles Smith,^{*} Hossein Askari,^{*} Geoffrey T. Struble,[†] Robyn Williams,[†] Sanjay Bhanot,[§] Brett P. Monia,[§] Shariff Bayoumy,[†] Eugene Grant,[†] Gary W. Caldwell,[†] Matthew J. Todd,[†] Yin Liang,^{*} Micheal D. Gaul,[†] Keith T. Demarest,^{*} and Margery A. Connelly^{*}

Cardiovascular and Metabolic Disease Research^{*} and Community of Research Excellence and Advanced Technology,[†] Janssen Pharmaceutical Companies of Johnson and Johnson, Spring House, PA 19477; ISIS Pharmaceuticals, Inc.,[§] Carlsbad, CA 92010

Abstract Diacylglycerol acyltransferase (DGAT) catalyzes the final step in triglyceride (TG) synthesis. There are two isoforms, DGAT1 and DGAT2, with distinct protein sequences and potentially different physiological functions. To date, the ability to determine clear functional differences between DGAT1 and DGAT2, especially with respect to hepatic TG synthesis, has been elusive. To dissect the roles of these two key enzymes, we pretreated HepG2 hepatoma cells with ¹³C₃-D₅-glycerol or ¹³C₁₈-oleic acid, and profiled the major isotope-labeled TG species by liquid chromatography tandem mass spectrometry. Selective DGAT1 and DGAT2 inhibitors demonstrated that ¹³C₃-D₅-glycerol-incorporated TG synthesis was mediated by DGAT2, not DGAT1. Conversely, ¹³C₁₈-oleoyl-incorporated TG synthesis was predominantly mediated by DGAT1. To trace hepatic TG synthesis and VLDL triglyceride (VLDL-TG) secretion in vivo, we administered D₅-glycerol to mice and measured plasma levels of D₅-glycerol-incorporated TG. Treatment with an antisense oligonucleotide (ASO) to DGAT2 led to a significant reduction in D₅-glycerol incorporation into VLDL-TG. In contrast, the DGAT2 ASO had no effect on the incorporation of exogenously administered ¹³C₁₈-oleic acid into VLDL-TG. Thus, our results indicate that DGAT1 and DGAT2 mediate distinct hepatic functions: DGAT2 is primarily responsible for incorporating endogenously synthesized FAs into TG, whereas DGAT1 plays a greater role in esterifying exogenous FAs to glycerol.—Qi, J., W. Lang, J. G. Geisler, P. Wang, I. Petrounia, S. Mai, C. Smith, H. Askari, G. T. Struble, R. Williams, S. Bhanot, B. P. Monia, S. Bayoumy, E. Grant, G. W. Caldwell, M. J. Todd, Y. Liang, M. D. Gaul, K. T. Demarest, and M. A. Connelly. **The use of stable isotope-labeled glycerol and oleic acid to differentiate the hepatic functions of DGAT1 and -2.** *J. Lipid Res.* 2012. 53: 1106–1116.

Supplementary key words diacylglycerol acyltransferase • triglyceride synthesis • very low density lipoprotein triglyceride • liquid chromatography tandem mass spectrometry • ¹³C₃-D₅-glycerol • ¹³C₁₈-oleic acid

Manuscript received 6 September 2011 and in revised form 2 April 2012.

Published, JLR Papers in Press, April 3, 2012

DOI 10.1194/jlr.M020156

Triglycerides (TGs) are the chief route of transport of dietary fat within chylomicrons and VLDLs, as well as the main form of fuel storage in adipose tissue. TGs are synthesized from one glycerol and three FA molecules, which are attached via ester bonds to the hydroxyl groups of the glycerol backbone. Two major diacylglycerol acyltransferase (DGAT) isozymes, DGAT1 and DGAT2, have been identified. Although both enzymes convert diacylglycerol to TG, they do not share similarity in either their nucleotide or amino acid sequences and have most probably arisen by convergent evolution (1, 2). Although there are some differences in their tissue distributions, both DGAT1 and DGAT2 are highly expressed in organs that synthesize large amounts of TG, such as the liver, adipose tissue, and small intestine (3).

Studies with genetically altered mice, as well as in vivo suppression of DGAT expression, indicate that both DGAT1 and DGAT2 play important roles in TG synthesis. DGAT1 knockout mice (DGAT1^{-/-}) have reduced tissue TG levels and exhibit increased sensitivity to insulin and leptin (4). In addition, they are resistant to high-fat diet-induced obesity as a result of an increase in their metabolic rates (4). In contrast, knockout mice lacking DGAT2 (DGAT2^{-/-}) are lipopenic and die soon after birth as a result of profound reductions in substrates for energy metabolism and impaired skin permeability (5). Hepatic suppression of DGAT2 with antisense oligonucleotides (ASOs) reduced hepatic TG content in rodents (6, 7), and reversed diet-induced hepatic steatosis and insulin resistance

Abbreviations: AGPAT, 1-acylglycerol-3-phosphate acyltransferase; ASO, anti-sense oligonucleotide; DGAT, diacylglycerol acyltransferase; ER, endoplasmic reticulum; FAF, FA-free; GPAT, glycerol-3-phosphate acyltransferase; HTMS, high-throughput mass spectrometry; i.v., intravenously; LC/MS/MS, liquid chromatography tandem mass spectrometry; MGAT2, monoacylglycerol acyltransferase-2; MRM, multi-reaction monitoring; PAP, phosphatidic acid phosphohydrolase; siRNA, small interfering RNA; TG, triglyceride.

¹To whom correspondence should be addressed.

e-mail: jqj@its.jnj.com

Copyright © 2012 by the American Society for Biochemistry and Molecular Biology, Inc.

in rats (7). Liu et al. (8) also reported that decreasing hepatic DGAT2 activity with ASO treatment resulted in decreased VLDL-TG secretion in both wild-type and ob/ob mice. On the other hand, DGAT1 ASO treatment did not block hepatic steatosis in rats fed a high-fat diet (7). Yamaguchi et al. (9) also showed that DGAT1 ASO treatment did not protect against hepatic TG accumulation induced by a methionine choline-deficient diet. The specific role of DGAT1 in hepatic TG synthesis and steatosis was recently reported using liver-specific DGAT1 knockout mice and hepatic DGAT1 ASO knockdown. DGAT1 was required for hepatic steatosis induced by a high-fat diet and prolonged fasting, which are both characterized by delivery of exogenous FAs to the liver (10). Nevertheless, all of these findings are based on hepatic and plasma TG parameters after chronic inhibition of DGAT1 or DGAT2.

Understanding the acute flux of metabolites, such as FA and glycerol, through DGAT1- versus DGAT2-mediated TG synthesis pathways is fundamental for attaining new insights into hepatic lipid metabolism. Previously, we reported a liquid chromatography tandem mass spectrometry (LC/MS/MS) method for measuring VLDL-TG following incorporation of exogenously administered $^{13}\text{C}_{18}$ -oleic acid and demonstrated significant inhibition of hepatic VLDL-TG secretion by a DGAT1 inhibitor in rats (11). To elucidate the role of DGAT2 in hepatic TG synthesis and VLDL-TG secretion, we developed an alternative approach using stable isotope-labeled glycerol substrates to trace TG synthesis, $^{13}\text{C}_3\text{-D}_5$ -glycerol for in vitro and D_5 -glycerol for in vivo studies. We combined the use of stable isotope-labeled oleic acid and glycerol to trace the metabolic flux of these substrates into different species of TG. Two chemically distinct DGAT2-selective inhibitors, DGAT2 small interfering RNAs (siRNAs), and a DGAT2 gene-specific ASO were employed to discern the differences between hepatic DGAT1- and DGAT2-mediated TG synthesis at the molecular level. We found that DGAT2 is primarily responsible for incorporating endogenously synthesized FAs into TG, whereas DGAT1 is largely responsible for esterifying exogenous FAs to glycerol.

MATERIALS AND METHODS

Materials and reagents

Ammonium formate, triolein, FA-free BSA (FAF-BSA), oleoyl CoA, and $^{13}\text{C}_{18}$ -oleic acid were purchased from Sigma-Aldrich (St. Louis, MO). 1,2-Dicapryl-*sn*-glycerol, internal standards A [1,3-ditetradecanoyl-2-(9Z-hexadecenoyl)-*sn*-glycerol-d5] and B [1,3-diheptadecanoyl-2-(10Z-heptadecenoyl)-*sn*-glycerol-d5] were obtained from Avanti Polar Lipids, Inc. (Alabaster, AL). Isopropyl alcohol, acetonitrile, and tetrahydrofuran were from EMD Chemicals, Inc. (Gibbstown, NJ). The DGAT1-selective inhibitor A-922500 (Abbott), chemical name: (1R, 2R)-2-[[4'-[[phenylamino]carbonyl]amino] [1,1'-biphenyl]4-yl]carbonyl] cyclopentanecarboxylic acid, was purchased from Tocris Bioscience (Ellisville, MO). The DGAT1-selective inhibitor JNJ-DGAT1-A, chemical name: N-[2,6-dichloro-4-(pyrrolidin-1-ylmethyl) phenyl]4-(4-[(4-methoxyphenyl)acetyl]amino)phenyl) piperazine-1-carboxamide, DGAT2-selective inhibitor JNJ-DGAT2-A, chemical name: 3-bromo-4-[2-fluoro-4-(4-oxo-2-[(2-pyridin-2-

ylethyl)amino]1,3-thiazol-5(4H)-ylidene)methyl]phenoxy] benzonitrile, and DGAT2-selective inhibitor JNJ-DGAT2-B, chemical name: 5-fluoro-2-(3-phenoxyphenyl)-1,2-benzisothiazol-3(2H)-one, were synthesized at Janssen Research and Development. $^{13}\text{C}_3\text{-D}_8$ -glycerol and D_8 -glycerol were purchased from Cambridge Isotope Laboratories (Cambridge, MA). Because three of the deuterated (D) oxygen atoms in $^{13}\text{C}_3\text{-D}_8$ -glycerol or D_8 -glycerol were readily exchangeable with hydrogen (H) in the buffer system (H_2O), we herein refer to the two substrates as $^{13}\text{C}_3\text{-D}_5$ -glycerol and D_5 -glycerol, respectively. Details regarding the DGAT2 mRNA-selective ASO inhibitor (ISIS-2177376) and a control ASO (ISIS-141923) were reported previously (6).

Screening for human DGAT2 inhibitors

Recombinant human DGAT2 was produced in a baculovirus expression system. Sf9 insect cells were infected for 72 h. Cell pellets were resuspended in homogenization buffer (0.1 M sucrose, 50 mM KCl, 40 mM KH_2PO_4 , 30 mM EDTA, pH 7.2) and homogenized. After centrifugation at 2,500 *g* for 15 min at 4°C, the pellet was resuspended in 500 ml lysis buffer, and total cell membranes were collected by ultracentrifugation at 100,000 *g* for 60 min at 4°C. The collected membranes were resuspended in homogenization buffer. DGAT2 catalyses the formation of TG using 1,2-dicapryl-*sn*-glycerol and oleoyl-CoA as substrates; therefore, the product carrying two capryl side chains and one oleoyl side chain, TG-(C10:0, C10:0, C18:1), was detected by high-throughput mass spectrometry (HTMS) in a 384-well format. Briefly, compounds were dispensed into wells of a 384-well polypropylene plate by a HummingbirdTM (Digilab Genomic Solutions, Inc.). DGAT2 activity was assayed in a solution containing 100 mM Tris-HCl (pH 7.5), 2 $\mu\text{g}/\text{ml}$ DGAT2-expressing membranes, 0.25 M sucrose, 15 mM MgCl_2 , 1 mM EDTA, 0.1% BSA, 25 μM oleoyl-CoA, and 25 μM 1,2-dicapryl-*sn*-glycerol diluted to 1% acetone, in a total reaction volume of 50 μl . The reaction was quenched with the addition of 50 μl 1N HCl. The reaction product was quantified by HTMS detection using a RapidFireTM system interfaced with a Sciex 4000 triple quadrupole through an atmospheric pressure chemical ionization source. The mass spectrometer was operated in the positive ion mode. A characteristic in-source fragment ion, *m/z* 493.8 from the product 1,2-dicapryl-3-oleoyl-glycerol, was detected. Data were reported as area under the product generation curve. A high-throughput screening campaign of 310,000 compounds using this HTMS assay yielded a hit rate of 0.3%, with the definition of a hit being greater than 65% inhibition at 7 μM .

LC/MS/MS-based assays for recombinant human DGAT1, DGAT2, and MGAT2 activity

Recombinant human DGAT1- or DGAT2-expressing Sf9 membranes were produced in a baculovirus expression system as previously described (11). DGAT activity was assayed in a solution containing 100 mM Tris-HCl (pH 7.5), 5 $\mu\text{g}/\text{ml}$ DGAT1- or DGAT2-expressing membranes, 0.25 M sucrose, 15 mM MgCl_2 , 1 mM EDTA, 0.1% BSA, 50 μM oleoyl-CoA, and 50 μM 1,2-dicapryl-*sn*-glycerol diluted to 1% acetone, in a total reaction volume of 100 μl for 40 min. The reaction mixture (20 μl) was quenched with the addition of 150 μl of 90% isopropyl alcohol and 10% tetrahydrofuran containing 20 nM of internal standard A. The reaction product, TG-(C10:0, C10:0, C18:1), was determined by LC/MS/MS. The LC/MS/MS system consisted of an Agilent 1100 Series liquid chromatographic system (Agilent Technologies; Palo Alto, CA) interfaced with a Micromass Quattro Micro triple quadrupole mass spectrometer (Waters; Milford, MA) through a Z-spray electrospray ionization source. The mass spectrometer was operated in the positive-ion mode. Separation of the analytes was carried out on a Eclipse XDB-C8 column

(2.1 × 50 mm) eluted isocratically with mobile phases A and B (60:40) at a flow rate of 0.3 ml/min. The mobile phase A was 5 mM ammonium formate in acetonitrile-water (95:5) and B was 5 mM ammonium formate in isopropyl alcohol-water (95:5). Quantitation of TG-(C10:0, C10:0, C18:1) was achieved in multi-reaction monitoring (MRM) mode. The ion transitions of m/z 682.8 $[M+NH_4]^+ \rightarrow 493.5$ and 771.8 $[M+NH_4]^+ \rightarrow 526.6$ at a collision energy of 20 eV were used for detection of TG-(C10:0, C10:0, C18:1) and internal standard A, respectively. Data were reported based on the relative peak areas to the internal standard.

The human monoacylglycerol acyltransferase-2 (MGAT2) activity was performed using microsomal membranes from Sf9 insect cells overexpressing human MGAT2 (12). MGAT2 activity was measured via LC/MS/MS detection of MGAT2-mediated formation of diacylglycerol.

Determination of the contribution of DGAT1 versus DGAT2 activity in HepG2 cell lysates

HepG2 cells were maintained in minimum essential medium with 2 mM L-glutamine, 1.5 g/l sodium bicarbonate, 0.1 mM non-essential amino acids, 1.0 mM sodium pyruvate, and 10% FBS. HepG2 cells were trypsinized and passed through a sterilized syringe to disperse cell aggregates. Cells were plated (45,000 cells/well) in a 96-well plate and assayed after reaching 50–60% confluence.

HepG2 cell monolayers were scraped in homogenization buffer (100 mM Tris-HCl, pH 7.5, 0.25 M sucrose, 15 mM MgCl₂, 1 mM EDTA) and homogenized by sonication. After centrifugation at 3,000 g for 15 min at 4°C, the supernatant was collected. DGAT activity was assayed in a solution containing 100 mM Tris-HCl (pH 7.5), 75 µg/ml HepG2 cell lysate, 0.25 M sucrose, 15 mM MgCl₂, 1 mM EDTA, 0.1% BSA, 50 µM oleoyl-CoA, and 50 µM 1,2-dicapryl-*sn*-glycerol diluted to 1% acetone in a total reaction volume of 100 µl for 40 min. Activity was measured in the presence or absence of a DGAT1 or DGAT2 inhibitor. Twenty microliters of the reaction was quenched with the addition of 150 µl of 90% isopropyl alcohol and 10% tetrahydrofuran containing 20 nM of the internal standard TG-(C14:0, C16:1, C14:0). The reaction product, TG-(C10:0, C10:0, C18:1) was determined by LC/MS/MS as described above.

Measurement of stable isotope-labeled TGs in HepG2 cells

For stable isotope labeling of TG using ¹³C₃-D₅-glycerol, HepG2 cells were washed once with PBS (pH 7.4) and incubated with DMEM supplemented with 25 mM HEPES (pH 7.5) (DMEM buffer) containing 0.1% FAF-BSA at 37°C for 15 min, followed by replacement with fresh DMEM buffer containing 0.1% FAF-BSA. DGAT1 or DGAT2 inhibitors were added to the cells in a concentration-dependent manner (0.3125, 0.625, 1.25, 2.5, 5, 10, and 20 µM) for a final DMSO concentration of 0.1%. Control wells received 0.1% DMSO alone. Cells were incubated at 37°C for 10 min. ¹³C₃-D₅-glycerol in DMEM buffer containing 0.1% FAF-BSA was added to each well for a final concentration of 20 µM. The plates were incubated for 2 h at 37°C, and the medium was removed. After briefly drying by air, 100 µl freshly prepared solvent (90% isopropyl alcohol and 10% tetrahydrofuran) containing 20 nM of internal standard B was added and allowed to sit at room temperature for 15 min with shaking. The extraction mixture (80 µl) was transferred to glass inserts in a 96-well deep-well plate. The plate was centrifuged at 3,000 rpm for 5 min, and the extracted samples were analyzed by LC/MS/MS (see details of LC/MS/MS analysis below). Percentage inhibition was calculated as 100-[(sample-low control)/(vehicle - low control) * 100] where low control is no addition of ¹³C₃-D₅-glycerol. A best-fit curve was fitted by a minimum sum-of-squares method to the

plot of % inhibition versus compound concentration using GraphPad Prism software.

For stable isotope labeling of TG using ¹³C₁₈-oleic acid, HepG2 cells were washed once with PBS and incubated with DMEM buffer containing 0.2% FAF-BSA at 37°C for 60 min. DGAT1 or DGAT2 inhibitors were added to cells in a concentration-dependent manner (between 1 nM and 1 µM), for a final DMSO concentration of 0.2%, in DMEM buffer containing 0.2% FAF-BSA. Cells were incubated with 0.2% DMSO or compound for 60 min. ¹³C₁₈-oleic acid, complexed with FAF-BSA in DMEM buffer containing 0.2% FAF-BSA, was added to each well for a final concentration of 150 µM. The plates were incubated for 2 h at 37°C, and the medium was removed. The ¹³C₁₈-oleoyl-labeled TGs were extracted and detected as previously described (11).

LC/MS/MS analyses of stable isotope-labeled TGs

Separation of the analytes was performed on an Agilent 1100 liquid chromatographic system using an Eclipse XDB-C₈ column (2.1 × 50 mm, particle size = 3.5 µm) and the same mobile phases as described above. The mobile phases were applied to generate a linear gradient elution as follows: 50–80% B in 5 min, hold 80% B for 1 min, return to 50% B in 0.1 min and a post-run time of 5 min. The flow rate was 0.3 ml/min, and sample injection volume was 3 µl. The Micromass Quattro Micro mass spectrometer was operated in the positive-ion MRM mode for the detection of a specific molecular mass transition m/z $(M+NH_4)^+ > [MNH_4 - (RCOOH+NH_3)]^+$ for each TG at a collision energy of 25 eV. Nitrogen was used as nebulizing gas and desolvation gas, and argon was used as collision gas. The MS source parameters were set as follows: capillary voltage, 3.1 kV; cone voltage, 25 V; extractor, 2V; RF lens, 0.1V; source temperature, 120°C; desolvation temperature, 300°C; cone gas flow, 50 l/hr; and desolvation gas flow, 700 l/hr. MassLynx software version 4.1 was used for system control and data processing.

Suppression of DGAT2 expression by siRNA in HepG2 cells

One day prior to transfection, HepG2 cells were trypsinized, passed through a sterile syringe, and seeded (200,000 cells/well) in a 24-well plate. DGAT2 silencer select pre-designed siRNAs (ID: S39247 and ID: 112270; designated DGAT2-siRNA A and DGAT2-siRNA B, respectively), and a control siRNA containing a scrambled sequence (Ambion, Austin, TX) were transfected by siPORT amine transfection agent (Ambion) according to the manufacturer's instructions. Forty-eight hours post-transfection, HepG2 cells were incubated with DMEM buffer containing 0.1% FAF-BSA at 37°C for 15 min. ¹³C₃-D₅-glycerol in DMEM buffer containing 0.1% FAF-BSA was added to each well at a final concentration of 30 µM. The plates were incubated for 2 h at 37°C before subsection to lipid extraction with 200 µl 90% isopropyl alcohol and 10% tetrahydrofuran containing 20 nM of internal standard B, followed by LC/MS/MS analysis. The mRNA levels of DGAT2 and GAPDH 48 h post siRNA transfection were measured using the Quantigene 2.0 branched DNA method following the directions provided by the manufacturer (Affymetrix; Santa Clara, CA).

DGAT2 ASO treatment in C57BL/6J mice

Adult male C57BL/6J mice with free access to water and standard laboratory rat chow were used in this study. The Institutional Animal Care and Use Committee of Janssen Pharmaceutical Companies of Johnson and Johnson approved all procedures. The sequences for the ASOs were as follows: DGAT2 ASO (ISIS-217376) 5'-TCCATTTATTAGTCTAGGAA-3' and control ASO (ISIS-141923) 5'-CCTTCCCTGAAGGTTCTCC-3'. In earlier studies, ISIS-217376 was shown to be a potent and specific

oligonucleotide for reducing DGAT2 mRNA levels (6). In addition, the control ASO does not have perfect complementarity to any known gene in public databases. The first five bases and last five bases of these ASOs have 2'-*O*-(2-methoxy)-ethyl modifications, and both have a phosphorothioate backbone. For these experiments, D₅-glycerol was diluted in saline and ¹³C₁₈-oleic acid was complexed with 10% FAF-BSA in saline. C57BL/6J mice fed standard chow diet (5001 Purina) were treated subcutaneously with 25 mg/kg DGAT2 ASO or control ASO twice a week for 3 weeks. Following ASO treatment, D₅-glycerol or ¹³C₁₈-oleic acid (10 mg/kg) was administered intravenously (i.v.). Blood was drawn via tail vein puncture and collected in a tube containing EDTA at the following time points: pretreatment, 15, 30, and 60 min post-treatment. Samples were centrifuged at 500 *g* for preparation of plasma. Plasma samples (10 μl) were transferred into glass inserts in a 96-well plate. An aliquot of 150 μl of extraction solvent (chloroform-methanol; 2:1; v/v) containing 0.2 μM internal standard B was added to each well and mixed. The 96-well plate was left at room temperature for 30 min and then centrifuged at 3,000 rpm for 10 min on a Beckman Allegra 6 centrifuge. The supernatant (100 μl) was transferred into a glass insert in another 96-well plate, and solvent was evaporated to dryness under a stream of nitrogen gas. The sample residues were reconstituted with 100 μl of solvent (isopropanol-tetrahydrofuran; 2:1; v/v) and mixed prior to LC/MS/MS analysis.

Quantitative real-time RT-PCR

Total RNA from HepG2 cells or mouse livers was isolated and transcribed using a high-capacity cDNA reverse transcription kit (Applied Biosystems; Foster City, CA). The cDNA was amplified with a SYBR Green PCR Master Mix (Applied Biosystems) on an Applied Biosystems Prism 7000 sequence detection system. Relative gene expression of DGAT1 or DGAT2 in HepG2 cells was calculated after normalization by 18S rRNA. RT-PCR data of DGAT2 mRNA in mouse livers were normalized to the total RNA abundance determined by RiboGreen RNA assay.

RESULTS

Identification of two potent, selective inhibitors of DGAT2

We identified two chemically distinct DGAT2 inhibitors, JNJ-DGAT2-A and JNJ-DGAT2-B, during a high-throughput screening campaign of 310,000 compounds (Table 1). The IC₅₀ values for JNJ-DGAT2-A and JNJ-DGAT2-B in an enzymatic assay using human DGAT2-expressing Sf9 membranes were 0.14 μM and 0.18 μM, respectively. Neither JNJ-DGAT2-A nor JNJ-DGAT2-B inhibited human DGAT1 or human MGAT2 at concentrations up to 10 μM (Table 1). In addition, JNJ-DGAT2-A and JNJ-DGAT2-B did not inhibit TG synthesis (up to 10 μM) in a human DGAT1 cell-based assay, where HEK293H cells were incubated with ¹³C₁₈-oleic acid, and ¹³C₁₈-oleoyl-incorporated TGs were quantified via LC/MS/MS (Table 1) (11). Furthermore, the incorporation of the ¹³C₁₈-oleoyl-substrate into TGs requires sequential enzymatic reactions catalyzed by multiple enzymes prior to the final DGAT-mediated step in the glycerol-3-phosphate pathway (11). However, JNJ-DGAT2-A and JNJ-DGAT2-B do not inhibit glycerol-3-phosphate acyltransferase (GPAT), 1-acylglycerol-3-phosphate acyltransferase (AGPAT), or phosphatidic acid phosphohydrolase (PAP)

TABLE 1. In vitro selectivity profile of two DGAT2 inhibitors

| | JNJ-DGAT2-A | JNJ-DGAT2-B |
|-------------------------|-----------------------------|-----------------------------|
| Enzyme assay | IC₅₀ (μM) | IC₅₀ (μM) |
| DGAT2 | 0.14 | 0.18 |
| DGAT1 | >10 | >10 |
| MGAT2 | >10 | >10 |
| Cell based assay | IC₅₀ (μM) | IC₅₀ (μM) |
| DGAT1 | >10 | >10 |

activity as measured in the DGAT1 HEK293 cell-based assay (11). Taken together, these data suggest that JNJ-DGAT2-A and -B are selective inhibitors of DGAT2 activity.

Determination of the relative contributions of DGAT1 and DGAT2 to overall DGAT activity in HepG2 cells

HepG2 hepatoma cells were found to express both DGAT1 and DGAT2 (13), and we confirmed the expression of both DGAT1 and DGAT2 mRNA in these cells (Fig. 1A). To determine the relative contributions of DGAT1 and DGAT2 to total DGAT activity in HepG2 cell lysates, we utilized a nonspecific assay that measured DGAT-mediated formation of TG using both 1,2-dicapryl-*sn*-glycerol and oleoyl-CoA as substrates. The product TG, 1,2-dicapryl-3-oleoyl-glycerol (C10:0, C10:0, C18:1), was quantified by LC/MS/MS. Recombinant DGAT1- and DGAT2-expressing membranes were tested first to ensure that the DGAT1 and DGAT2 inhibitors were selective in their inhibitory profiles. When tested at a concentration of 5 μM, JNJ-DGAT2-A and JNJ-DGAT2-B inhibited about 99% of recombinant DGAT2 enzymatic activity, while the two DGAT1 inhibitors, JNJ-DGAT1-A (11) and A-922500 (14) tested at 1 μM, exhibited no inhibitory activity (data not shown). Conversely, when tested at a concentration of 1 μM, JNJ-DGAT1-A and A-922500 inhibited about 99% of recombinant DGAT1 enzymatic activity, whereas the two DGAT2 inhibitors, JNJ-DGAT2-A and JNJ-DGAT2-B, (5 μM) exhibited no inhibitory activity (data not shown). Therefore, we were confident that these inhibitors could be used to determine the relative contribution of DGAT1 and DGAT2 to total DGAT activity in HepG2 cell lysates. JNJ-DGAT1-A, A-922500, JNJ-DGAT2-A, and JNJ-DGAT2-B were tested alone or in combination in HepG2 lysates using both 1,2-dicapryl-*sn*-glycerol and oleoyl-CoA as substrates and quantifying the product TG, 1,2-dicapryl-3-oleoyl-glycerol (C10:0, C10:0, C18:1). The resulting data suggested that approximately 85% of DGAT activity in HepG2 lysates was mediated by DGAT1 and 20–30% was mediated by DGAT2 (Fig. 1B).

Analysis of the major TG species in HepG2 cells using ¹³C₃-D₅-glycerol as a substrate

Conventional cell-based TG synthesis assays use radio-labeled glycerol or FAs to metabolically label TG molecules. The radio-labeled hydrophobic TG product is typically resolved by TLC (1, 2). However, LC/MS/MS is

becoming the preferred method for quantitative lipid analysis due to the ease of automation, accuracy, and sensitivity, and the avoidance of radioactivity. We developed a high-throughput LC/MS/MS-based cellular assay for determining cellular DGAT activity using $^{13}\text{C}_3\text{-D}_5\text{-glycerol}$ in lieu of radio-labeled glycerol. In HepG2 cells, the exogenously added $^{13}\text{C}_3\text{-D}_5\text{-glycerol}$ was incorporated into the glycerol-3-phosphate pathway (Fig. 2A). After one-step extraction, the major species of $^{13}\text{C}_3\text{-D}_5\text{-glycerol}$ -incorporated TG species was detected by LC/MS/MS. We removed the exogenous FAs from the growth medium by washing and briefly incubating HepG2 cells in a FAF medium. Furthermore, the cell assay was performed in FAF, serum-free medium. Although all of the TG species were routinely measured, the five major $^{13}\text{C}_3\text{-D}_5\text{-TG}$ species were reported, inasmuch as they appeared to consistently represent the overall changes observed in the TG pool. To clarify the terminology, $^{13}\text{C}_3\text{-D}_5\text{-TG}$ (52:2) refers to a TG containing 52 carbon atoms and 2 double bonds in the side chains of the FAs attached to

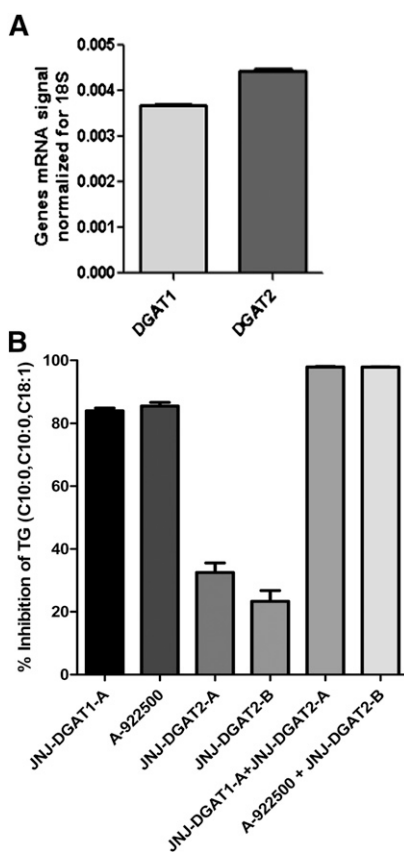


Fig. 1. A: Quantification of DGAT1 and DGAT2 mRNA levels by RT-PCR and normalization to the amount of 18S rRNA in HepG2 cells. B: Inhibition of diacylglycerol acyltransferase activity in HepG2 cell lysates by DGAT1 and DGAT2 inhibitors. [JNJ-DGAT1-A (1 μM), A-922500 (1 μM), JNJ-DGAT2-A (5 μM), JNJ-DGAT2-B (1 μM), JNJ-DGAT1-A (1 μM) + JNJ-DGAT2-A (5 μM), or A-922500 (1 μM) + JNJ-DGAT2-B (5 μM) were incubated with HepG2 cell lysates. The concentration of TG, 1,2-dicapryl-3-oleoyl-glycerol (C10:0, C18:1), was determined by LC/MS/MS. The percent inhibition was plotted as a surrogate for determining the amount of DGAT1 versus DGAT2 activity in HepG2 cells. Values represent the average of four data points \pm SD.

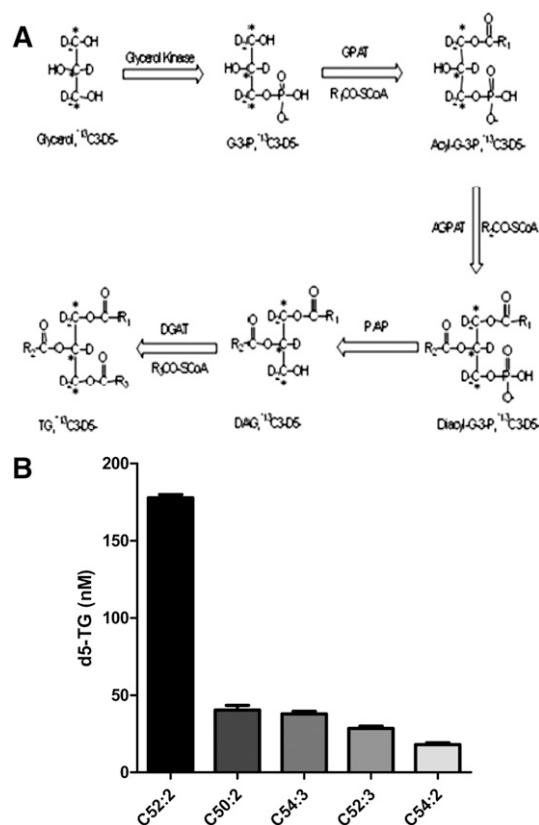


Fig. 2. A: Illustration of the glycerol-3-phosphate pathway whereby $^{13}\text{C}_3\text{-D}_5\text{-glycerol}$ is incorporated into the glycerol backbone of each TG molecule. The enzymes in this pathway include: glycerol kinase, glycerol-3-phosphate acyltransferase (GPAT), acylglycerophosphate acyltransferase (AGPAT), phosphatidic acid phosphohydrolase (PAP), and diacylglycerol acyltransferase (DGAT). B: HepG2 cell lysates were incubated for 2 h with heavy labeled glycerol, $^{13}\text{C}_3\text{-D}_5\text{-glycerol}$. After incubation, the five major species of TG (C52:2, C50:2, C54:3, C52:3, C54:2) were quantified via LC/MS/MS. Values represent the average of two data points \pm SD.

the labeled glycerol backbone. Following incubation of the HepG2 cells for 2 h with the heavy labeled substrate ($^{13}\text{C}_3\text{-D}_5\text{-glycerol}$), the relative abundance for these five major $^{13}\text{C}_3\text{-D}_5\text{-TG}$ species as determined by LC/MS/MS were: $^{13}\text{C}_3\text{-D}_5\text{-TG}$ (52:2) $>$ $^{13}\text{C}_3\text{-D}_5\text{-TG}$ (50:2) \sim $^{13}\text{C}_3\text{-D}_5\text{-TG}$ (54:3) $>$ $^{13}\text{C}_3\text{-D}_5\text{-TG}$ (52:3) $>$ $^{13}\text{C}_3\text{-D}_5\text{-TG}$ (54:2) (Fig. 2B). The relative abundance of these five $^{13}\text{C}_3\text{-D}_5\text{-TG}$ species varied slightly depending on differences in the cell culture conditions (e.g., in the presence or absence of serum in the medium), which is why we minimized the amount of exogenous FAs before and during the assay. In addition, we noted differences in the predominant TG species when different cell types were used for the assay (e.g., HepG2 versus primary rat hepatocytes versus McArdle-RH7777), which may reflect subtle differences in how cultured hepatocytes synthesize TGs. To validate the specificity of LC/MS/MS detection of $^{13}\text{C}_3\text{-D}_5\text{-TG}$ species, we incubated 20 μM D₅-glycerol or $^{13}\text{C}_3\text{-glycerol}$ or nonlabeled glycerol with HepG2 cells and observed that less than 2% of the LC/MS/MS signals corresponded to the mass transitions of all five $^{13}\text{C}_3\text{-D}_5\text{-TG}$ species.

Inhibition of DGAT2, but not DGAT1, significantly reduced the synthesis of stable isotope-labeled TG using $^{13}\text{C}_3\text{-D}_5$ -glycerol as a substrate in HepG2 cells

To determine the effects of DGAT2 inhibition on TG synthesis in HepG2 cells, the cells were preincubated in the presence and absence of one of the two DGAT2 inhibitors, JNJ-DGAT2-A and JNJ-DGAT2-B, or one of two DGAT1 inhibitors, JNJ-DGAT1-A and A-922500 (14), followed by incubation with the $^{13}\text{C}_3\text{-D}_5$ -glycerol substrate. JNJ-DGAT2-A dose-dependently inhibited the generation of the three major TG species with IC_{50} values of 0.85 μM , 0.99 μM , and 0.66 μM as calculated by the inhibition of formation of $^{13}\text{C}_3\text{-D}_5\text{-TG}$ (52:2), $^{13}\text{C}_3\text{-D}_5\text{-TG}$ (54:3), and $^{13}\text{C}_3\text{-D}_5\text{-TG}$ (50:2), respectively (Fig. 3A). Similarly, JNJ-DGAT2-B inhibited the production of the total of all five $^{13}\text{C}_3\text{-D}_5\text{-TG}$ species with an IC_{50} value of 1.6 μM (Fig. 3B). In contrast, neither of the two DGAT1-selective inhibitors, JNJ-DGAT1-A and A-922500, inhibited the synthesis of $^{13}\text{C}_3\text{-D}_5$ -glycerol-labeled TGs (Fig. 3B).

As a further means to investigate the effects of a reduction in DGAT2 activity on TG synthesis, we performed siRNA knockdown of DGAT2 mRNA expression in HepG2 cells. The DGAT2 mRNA levels were reduced 54.8%, 67.3%, and 76.1% by treatment with DGAT2 siRNA-A, DGAT2 siRNA-B, and a combination of both DGAT2 siRNA-A and DGAT2 siRNA-B, respectively (data not shown). Suppression of DGAT2 expression in HepG2 cells with either DGAT2 siRNA-A, DGAT2 siRNA-B, or both siRNAs combined significantly inhibited TG synthesis, as evidenced by a decrease in $^{13}\text{C}_3\text{-D}_5$ (52:2) (Fig. 4A), $^{13}\text{C}_3\text{-D}_5\text{-TG}$ (54:3) (Fig. 4B), and $^{13}\text{C}_3\text{-D}_5\text{-TG}$ (50:2) (Fig. 4C).

Inhibition of DGAT1, but not DGAT2, significantly reduced the synthesis of stable isotope-labeled TG using $^{13}\text{C}_{18}$ -oleic acid as a substrate in HepG2 cells

To test whether DGAT2 inhibition affected TG synthesis using $^{13}\text{C}_{18}$ -oleic acid as a substrate, HepG2 cells were incubated with $^{13}\text{C}_{18}$ -oleic acid. In this reaction, $^{13}\text{C}_{18}$ -oleic acid is converted to $^{13}\text{C}_{18}$ -oleoyl-CoA ($\text{H}_{33}\text{C}_{17}\text{CO-SCoA}$) before entering the glycerol-3-phosphate pathway (Fig. 5A). HepG2 cells were preincubated for 60 min in the presence and absence of the inhibitor JNJ-DGAT2-A prior to the addition of $^{13}\text{C}_{18}$ -oleic acid. Unlike the inhibition observed with $^{13}\text{C}_3\text{-D}_5$ -glycerol as a substrate, no inhibition of TG synthesis was observed with $^{13}\text{C}_{18}$ -oleic acid as a substrate, as evidenced by the lack of reduction in the predominant $^{13}\text{C}_{18}$ -oleic acid-incorporated TG species (stable isotope-labeled triolein; $^{13}\text{C}_{18}$ -oleoyl, $^{13}\text{C}_{18}$ -oleoyl, $^{13}\text{C}_{18}$ -oleoyl) (Fig. 5B). In contrast, exposure of HepG2 cells to JNJ-DGAT1-A and A-922500 resulted in dose-dependent inhibition of TG synthesis (stable isotope-labeled triolein; $^{13}\text{C}_{18}$ -oleoyl, $^{13}\text{C}_{18}$ -oleoyl, $^{13}\text{C}_{18}$ -oleoyl) (Fig. 5B). Based on the internal standard, the absolute amount of stable isotope-labeled triolein was approximately 1 to 2 orders higher than the combined $^{13}\text{C}_3\text{-D}_5$ -glycerol-incorporated major TG species in HepG2 cells.

Inhibition of stable isotope-labeled glycerol incorporation into VLDL-TG in DGAT2 ASO-treated mice

JNJ-DGAT2-A and JNJ-DGAT2-B exhibited inadequate metabolic stability in a liver microsome assay *in vitro*,

suggesting that they would not be useful for inhibition of hepatic DGAT activity *in vivo*. Therefore, we used a DGAT2 ASO to selectively reduce hepatic DGAT2 expression in C57BL/6J mice to interrogate the role of hepatic DGAT2 *in vivo*. DGAT2 ASO treatment, 25 mg/kg twice a week for 3 weeks, in C57BL/6J mice fed a standard chow diet resulted in a 70% reduction in the levels of hepatic DGAT2 mRNA (Fig. 6A) when compared with vehicle or control ASO-treated mice. To assess TG synthesis *in vivo*, C57BL/6J mice treated with 25 mg/kg DGAT2 or control ASO twice weekly for 3 weeks were administered a bolus dose of 10 mg/kg D_5 -glycerol, and plasma samples from treated mice were analyzed for D_5 -glycerol incorporation into

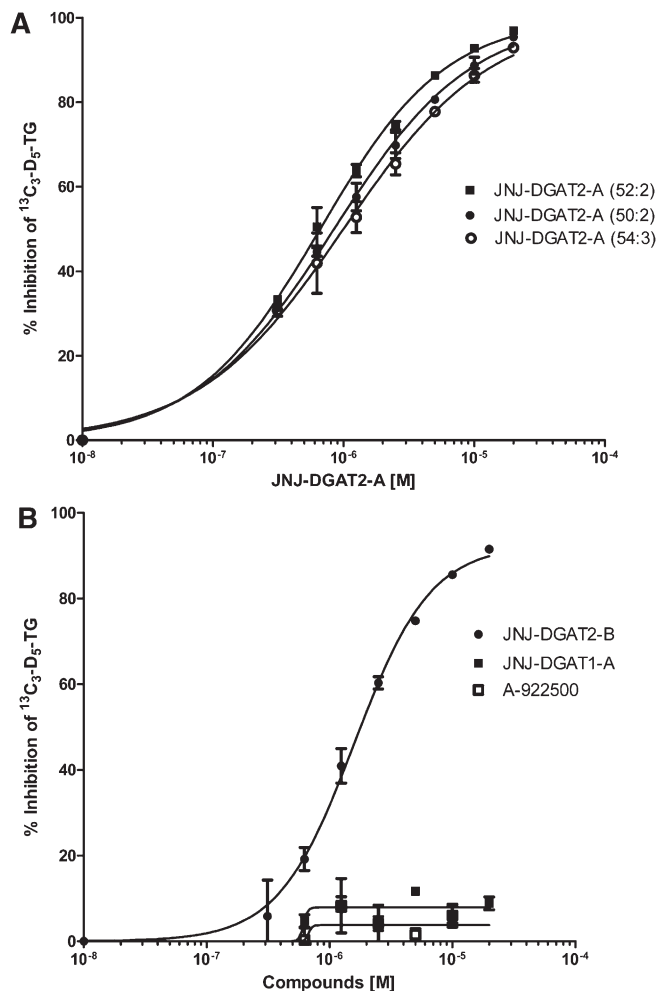


Fig. 3. Effects of DGAT2 and DGAT1 inhibitors on the incorporation of $^{13}\text{C}_3\text{-D}_5$ -glycerol in TGs synthesized in HepG2 cells. A: Increasing concentrations (0.3125, 0.625, 1.25, 2.5, 5, 10, and 20 μM) of JNJ-DGAT2-A were incubated with HepG2 cell lysates for 60 min prior to the addition of heavy labeled glycerol, $^{13}\text{C}_3\text{-D}_5$ -glycerol, and then incubated for an additional 2 h. Three of the five major TG species (C52:2, C50:2, C54:3) were quantified via LC/MS/MS. B: Increasing concentrations (0.3125, 0.625, 1.25, 2.5, 5, 10, and 20 μM) of JNJ-DGAT2-B, JNJ-DGAT1-A, and A-922500 were incubated with HepG2 cell lysates for 60 min prior to the addition of heavy labeled glycerol, $^{13}\text{C}_3\text{-D}_5$ -glycerol, and then incubated for an additional 2 h. The most-abundant TG species (C52:2) was quantified via LC/MS/MS. Values represent the average of two data points \pm SD.

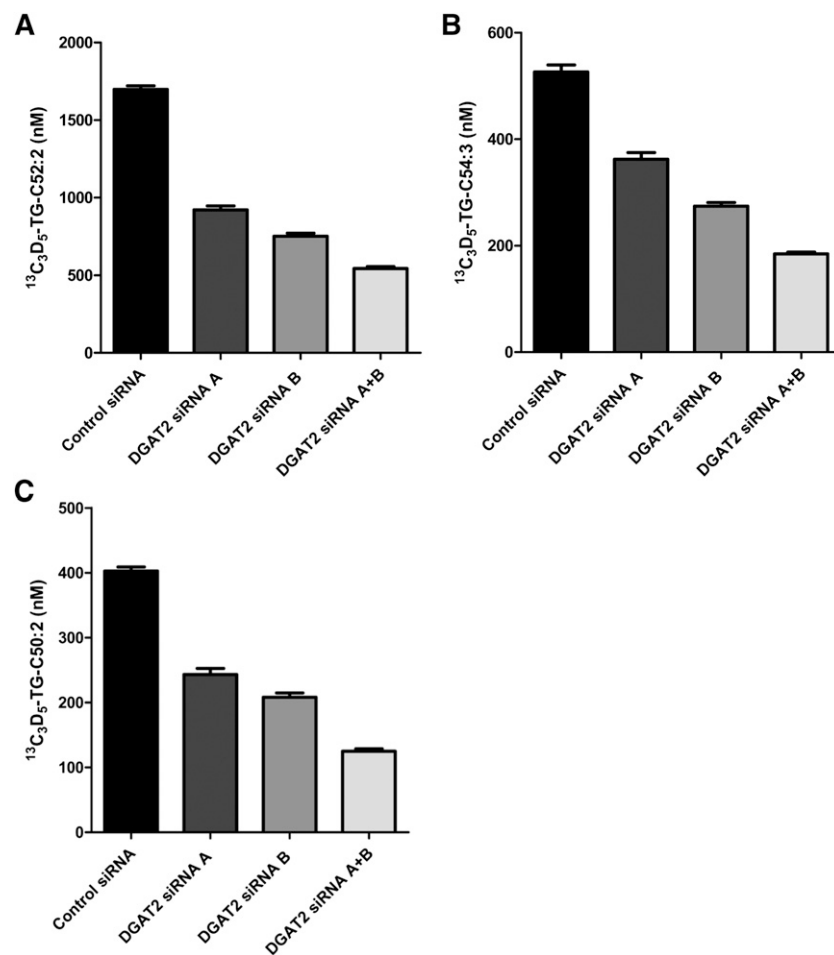


Fig. 4. Reduced incorporation of $^{13}\text{C}_3\text{-D}_5\text{-glycerol}$ into the major TG species synthesized in HepG2 cells after reduction of DGAT2 expression. DGAT2 siRNA A, DGAT2 siRNA B, and DGAT2 siRNA A + DGAT2 siRNA B were used to reduce the amount of DGAT2 expressed in HepG2 cells. Subsequently HepG2 cell lysates were incubated with heavy glycerol, $^{13}\text{C}_3\text{-D}_5\text{-glycerol}$, for 2 h. The three most-abundant TG species was quantified via LC/MS/MS. A: C52:2; B: C54:3; C: C50:2. Values represent the average of three data points \pm SD.

mostly VLDL-TG by LC/MS/MS analysis. $\text{D}_5\text{-TG}$ (52:2) accounted for about 70% of all the detected $\text{D}_5\text{-glycerol}$ -incorporated TG species combined. Therefore, we used $\text{D}_5\text{-TG}$ (52:2) as a surrogate for total $\text{D}_5\text{-glycerol}$ -incorporated VLDL-TG. $\text{D}_5\text{-TG}$ (52:2) peaked at 30 min, and dropped significantly by 60 min. There was a significant reduction in plasma VLDL-TG in mice treated with the DGAT2 ASO when compared with plasma from control ASO-treated mice (Fig. 6B, C). There were no differences in endogenous plasma levels of TG (52:2) between the control ASO- and DGAT2 ASO-treated groups (Fig. 6D). Notably, endogenous TG levels decreased from pretreatment levels over time in both treatment groups, possibly due to stress-related plasma TG metabolism.

Lack of inhibition of stable isotope-labeled oleic acid incorporation into VLDL-TG in DGAT2 ASO-treated mice

As previously reported, DGAT1 inhibition significantly reduced the incorporation of stable isotope-labeled oleic acid into VLDL-TG in vivo (11). To interrogate the role of DGAT2 in the incorporation of oleic acid into VLDL-TG

in vivo, we assessed the effects of the DGAT2 ASO on $^{13}\text{C}_{18}$ -oleic acid incorporation into VLDL-TG. C57BL/6J mice were treated with 25 mg/kg DGAT2 or control ASO twice weekly for 3 weeks prior to i.v. administration of stable isotope-labeled oleic acid, $^{13}\text{C}_{18}$ -oleic acid. There were no significant differences in $^{13}\text{C}_{18}$ -oleoyl-incorporated VLDL-TG between the control ASO- and DGAT2 ASO-treated animals, despite detection of a significant amount of $^{13}\text{C}_{18}$ -oleoyl-incorporated VLDL-TG (Fig. 7). Thus, in contrast to DGAT1 inhibition, a reduction in hepatic DGAT2 expression did not have an effect on exogenously administered $^{13}\text{C}_{18}$ -oleic acid incorporated into VLDL-TG.

DISCUSSION

In the liver, FAs may come from exogenous sources such as dietary fat or mobilization from white adipose tissue during fasting. Alternatively, FAs can arise from endogenous de novo synthesis. Both DGAT1 and DGAT2 are highly expressed in the liver (1, 2), and both are involved in the terminal, committed step of TG synthesis. A recent

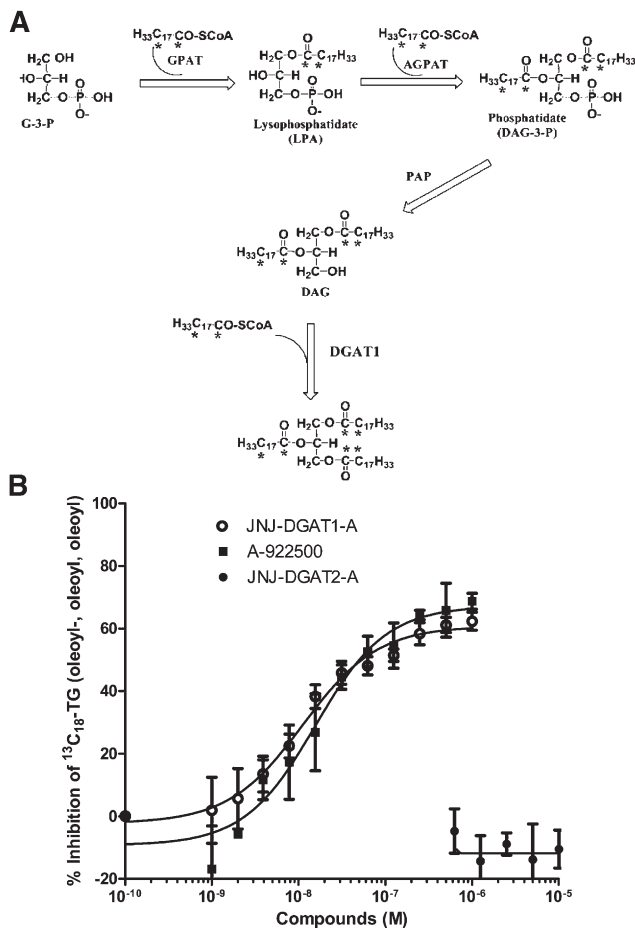


Fig. 5. A: Illustration of the incorporation of ¹³C₁₈ oleic acid into TG in the glycerol-3-phosphate pathway. B: Effect of DGAT1 and DGAT2 inhibitors on the incorporation of ¹³C₁₈ oleic acid into triolein synthesized in HepG2 cells. Increasing concentrations of JNJ-DGAT1-A and A-922500 (between 1 nM and 1 μM) and JNJ-DGAT2-A (0.625, 1.25, 2.5, 5, and 10 μM) were incubated with HepG2 cell lysates for 60 min prior to the addition of heavy labeled oleic acid and ¹³C₁₈ oleic acid, and then incubated for an additional 2 h. The amount of triolein, ¹³C₁₈-TG (oleoyl-, oleoyl-, oleoyl) was quantified via LC/MS/MS. Values represent the average of three data points ± SD.

elegant study using global and liver-specific inactivation of DGAT1 in mice demonstrated that DGAT1 plays a specific role in the development of hepatic steatosis resulting from exogenous FAs but not from endogenous FA synthesis (10). On the other hand, the functional role of DGAT2 in bulk hepatic TG synthesis has been well established in mice and rats (6, 7). In the present study, we identified two chemically distinct DGAT2 inhibitors, JNJ-DGAT2-A and JNJ-DGAT2-B. These inhibitors, as well as previously characterized DGAT1 inhibitors, allowed us to determine that DGAT1 is responsible for the majority (85%) of total DGAT activity in HepG2 cell lysates (11). The remaining DGAT activity in HepG2 cells appears to be DGAT2-mediated (20–30%). Our data are consistent with previously reported data on DGAT1 activity in HepG2 cells (15). To further define potential differences in the hepatic functions of DGAT1 and DGAT2, we investigated TG synthesis in human HepG2 cells and in C57BL/6j mice using stable

isotope-labeled oleic acid and glycerol as tracers to measure TG metabolism.

Previously, we reported an LC/MS/MS method in which we employed stable isotope-labeled oleic acid, ¹³C₁₈-oleic acid, to monitor the cellular glycerol-3-phosphate pathway in HEK293 cells and VLDL-TG secretion in rats. ¹³C₁₈-oleic acid was recently used to elucidate lipid assembly *in vivo* by measuring the plasma labeling pattern of TG, phospholipids, and cholesteryl esters (16). Here, we utilized two potent, selective DGAT2 inhibitors to interrogate the role of DGAT2 in ¹³C₁₈-oleic acid incorporation into TG in HepG2 cells. Results confirmed the hypothesis that DGAT1, but not DGAT2, is primarily responsible for esterification of exogenous FAs (exogenously added ¹³C₁₈-oleic acid) to the glycerol backbone. Notably, the maximum DGAT1-mediated inhibition of ¹³C₁₈-oleic acid-incorporated TG (stable isotope-labeled triolein) was about 70% using two DGAT1-selective inhibitors representing different chemotypes. Furthermore, we reported that hepatic DGAT1 inhibition was associated with significant inhibition of ¹³C₁₈-oleoyl incorporation into newly synthesized VLDL-TG post ¹³C₁₈-oleic acid administration in rats (11). In contrast, we now report that reduction in hepatic DGAT2 expression in mice with a DGAT2-specific ASO did not affect the incorporation of ¹³C₁₈-oleic acid into newly synthesized VLDL-TG when measured acutely, before equilibration into the endogenous TG pools. Therefore, the use of LC/MS/MS-based measurement of ¹³C₁₈-oleic acid as a tracer of newly synthesized TG confirms the role of DGAT1 in esterifying exogenous FAs into hepatic VLDL-TG *in vivo*.

Here, we report the development of a high-throughput, LC/MS/MS-based cellular TG synthesis assay using heavy labeled glycerol, ¹³C₃-D₅-glycerol, as a substrate instead of radio-labeled glycerol. To eliminate the majority of unlabeled exogenous FAs, we removed FAs from the cell growth medium before adding stable isotope-labeled glycerol to HepG2 cells. Thus, the use of stable isotope-labeled glycerol to measure TG synthesis allows incorporation of FAs that arise predominantly from the endogenous pool. In contrast to the incorporation of ¹³C₁₈-oleic acid in TG synthesis, we demonstrated that ¹³C₃-D₅-glycerol-incorporated TG synthesis is largely mediated by DGAT2 but not DGAT1 *in vitro* in HepG2 cells. These results agree with two previous reports in which RNAi knock-down of DGAT2 in primary rat and mouse hepatocytes significantly reduced the amount of radio-labeled glycerol incorporated into the endogenous pool of TG (6, 7). In our studies, the most-abundant ¹³C₃-D₅-glycerol-incorporated TG species detected is ¹³C₃-D₅ (52:2) in HepG2 cells (Fig. 2B) and rat primary hepatocytes (data not shown). Based on the natural abundance of mammalian TG, we postulate that ¹³C₃-D₅ (52:2) is represented by ¹³C₃-D₅-TG-containing oleoyl, palmitoyl, and oleoyl chains. We estimated that the absolute amount of ¹³C₁₈-oleic acid-labeled triolein, based on the internal standard, to be 1- to 2-fold higher than ¹³C₃-D₅-glycerol-incorporated major TG species combined in HepG2 cells. This implies that exogenous oleic acid drives more TG synthesis than

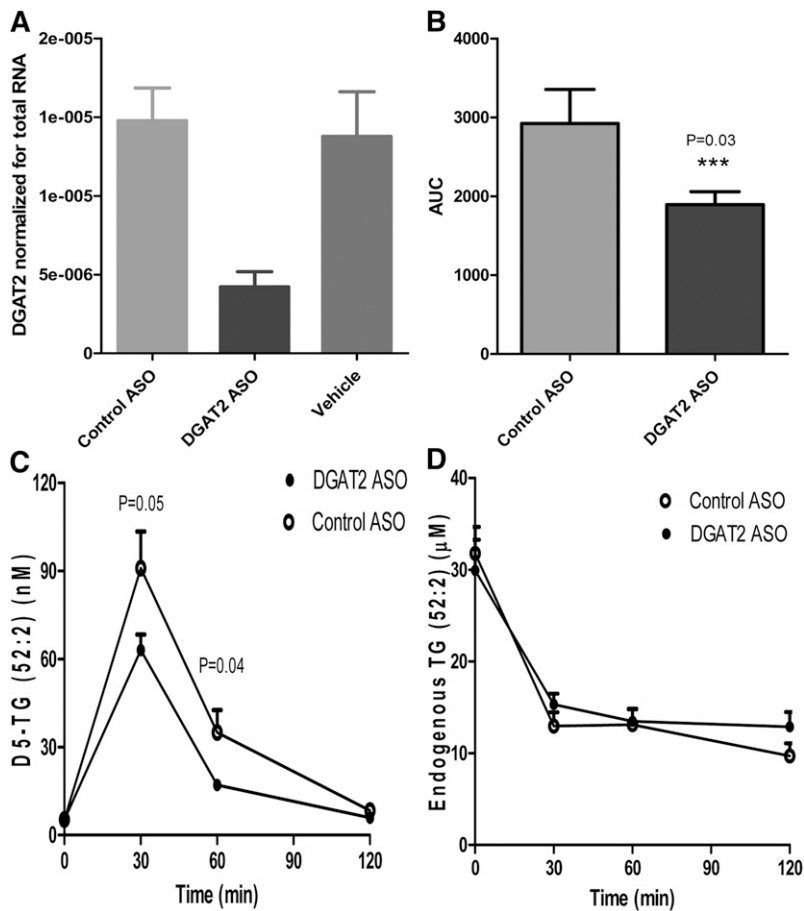


Fig. 6. Effects of reduction in hepatic DGAT2 expression in mice by DGAT2 ASO on incorporation of D₅-glycerol into plasma VLDL-TG. **A:** Liver expression of DGAT2 was measured via quantitative PCR after 3 weeks treatment in C57BJ6 mice with either a control ASO, a DGAT2-specific ASO, or vehicle alone. RT-PCR data of DGAT2 mRNA were normalized to the total RNA abundance determined by RiboGreen RNA assay. **B and C:** Time course of D₅-glycerol-incorporated VLDL-TG (D5-TG, 52:2) in mice treated with either a DGAT2-specific or a control ASO. Results expressed as area under the curve and in graph form. **D:** Time course of endogenous TG-incorporated VLDL-TG (TG, 52:2) in mice treated with either a DGAT2-specific or a control ASO. Data are expressed as mean values ± SEM of 10 animals in each group.

endogenous FA-incorporated TG synthesis in this hepatoma cell line.

Stable isotope-labeled glycerol has been used to measure the kinetics of VLDL-TG secretion and metabolism *in vivo* (17, 18). However, these methods required isolation of VLDL-TG by TLC and necessitate hydrolysis of the samples in order to release the glycerol. Labeled VLDL-TG is typically quantified by indirect measurement of the derivatized stable isotope-labeled glycerol by GC/MS. By using LC/MS/MS to directly detect and quantify the major stable isotope-labeled TG species, we found that the incorporation of the stable isotope-labeled glycerol into VLDL-TG peaked around 30 min in rats (data not shown) and mice (reported here), similar to previous reports (17, 18). We demonstrated that the flux of stable isotope-labeled glycerol-incorporated VLDL-TG in mice is mediated largely by DGAT2 and not DGAT1. Therefore, the use of LC/MS/MS-based measurement of D₅-glycerol as a tracer of newly synthesized TG confirms the role of DGAT2 in esterifying FAs into hepatic VLDL-TG *in vivo*. Notably, there are limitations to measuring the incorporation of heavy labeled substrates in liver TGs, at least within the timeframe of our assays. We attempted to detect the incorporation of ¹³C₁₈ oleic acid into TG in the liver. Because of the large existing pool of unlabeled TGs in the liver when compared with plasma, the percentage of ¹³C₁₈-oleic acid-incorporated TG was estimated to be only 0.2% of the total hepatic TG pool versus approximately 2% of the total TG pool in the plasma. Furthermore, we could not detect D₅-glycerol-incorporated

TG in the liver by LC/MS/MS due to overwhelming endogenous hepatic TG content.

The most-intriguing finding from these studies relates to the ability of DGAT1 inhibitors to block incorporation of exogenously added oleate but not to disrupt incorporation of exogenously added glycerol into TG, and the opposite is true for the selective DGAT2 inhibitors. In other words, DGAT2 preferentially esterifies exogenously added glycerol to endogenously synthesized FAs, and DGAT1 preferentially esterifies exogenously added oleic acid to

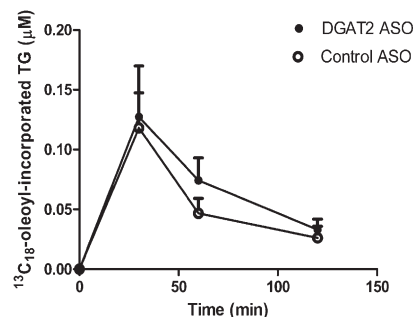



Fig. 7. Effects of reduction in hepatic DGAT2 expression in mice by DGAT2 ASO on incorporation of ¹³C₁₈ oleic acid into plasma VLDL-TG. Time course of ¹³C₁₈ oleic acid-incorporated VLDL-TG in mice treated with either a DGAT2-specific or a control ASO. The amount of triolein, ¹³C₁₈-TG (oleoyl-, oleoyl-, oleoyl-), was quantified via LC/MS/MS. Data are expressed as mean values ± SEM of five animals in each group.

already-existing diacylglycerol. We believe that there are at least two potential explanations for these observations. Both of these hypotheses rely on the assumption that DGAT1 and DGAT2 reside in different, very specialized compartments within the endoplasmic reticulum (ER). The first hypothesis is one of differential trafficking. One could speculate that the glycerol substrate, when added exogenously, is trafficked to a cellular compartment that is accessible to DGAT2, but not DGAT1. It then follows that exogenously added oleic acid substrate is trafficked to a cellular compartment that is readily accessible to DGAT1, but not DGAT2 activity. Experiments to prove or disprove this hypothesis would be very difficult, given the complexities of cellular trafficking and the fact that there is so much we do not understand regarding lipid trafficking to date. The second hypothesis is that other enzymes within the glycerol phosphate pathway (glycerol kinase, GPAT, AGPAT and/or PAP) are also compartmentalized. For example, we know that DGAT2 and SCD1 reside near each other in the ER. Glycerol kinase, GPAT, AGPAT and/or PAP may also reside within a cellular compartment that contains DGAT2 and SCD1, but not DGAT1. In this case, exogenously delivered glycerol and oleic acid would traffic to either of the specialized ER compartments, but the enzymes within each compartment would determine their fates. For example, glycerol kinase may reside closer to the ER compartment containing DGAT2, thereby allowing DGAT2 access to diacylglycerol that has been synthesized using exogenously added glycerol and FAs that may have been processed by SCD1. Conversely, the compartment containing DGAT1 may have a predetermined pool of phosphorylated glycerol, allowing DGAT1 to efficiently synthesize TG from DAG that has been esterified using exogenously added FAs. This supports the idea that hepatic DGAT1 is predominantly responsible for esterification of exogenously added FAs and is therefore very efficient at processing and storage of dietary FAs. It also supports the supposition that DGAT2 is predominantly responsible for TG that is synthesized during de novo lipogenesis and is therefore very efficient at processing DAG that is immediately delivered from glycerol kinase, GPAT, AGPAT and PAP. This latter hypothesis is particularly attractive for two reasons: 1) In our assays the utilization of the heavy labeled substrates is measured within a fairly short timeframe (0.5–2 h). This short timeframe may not allow for the efficient movement of glycerol or DAG synthesized from one ER compartment, or hydrolyzed from a lipid droplet, to move to a second compartment where DGAT1 resides. Therefore, we are measuring immediate events in lipid processing; events that occur before a significant amount of re-compartmentalization or re-equilibration. 2) This hypothesis is congruous with other observations that have been previously published regarding selective compartmentalization of DGAT1 and DGAT2 and the differences in their function (8, 10, 19). We believe these assays will help future studies in tissues besides the liver that express both of these enzymes.

In liver, a fraction of newly synthesized TG is incorporated into secreted VLDL particles immediately after synthesis

and the rest is incorporated into the cytosolic pool for storage. One unresolved question is whether DGAT1 or DGAT2 catalyzes TG synthesis on the luminal surface of the ER. Several studies have reported that two separate DGAT activities are present in hepatic microsomes: an “overt” (cytosolic) activity and a “latent” (luminal) activity that appears after permeabilization (20, 21). The overt DGAT activity on the cytoplasmic side of the ER is thought to synthesize TG destined for deposition into cytosolic lipid droplets. The latent DGAT activity within the ER lumen is postulated to synthesize TG bound for VLDL-TG secretion (20, 21). Using stable isotope-labeled oleic acid or glycerol to trace hepatic VLDL-TG synthesis in rodents, we observed that the peak of newly synthesized VLDL-TG occurred about 30 min after the administration of the tracers, suggesting that fractions of newly synthesized TGs were readily secreted after synthesis, similar to previous studies (17, 18). Finally, our observations that hepatic reduction in DGAT1 and DGAT2 activity affects the exogenous oleic acid- or glycerol-incorporated VLDL-TG within a short period of time after substrate addition suggest that both DGAT1 and DGAT2 are involved in the synthesis of the TG pool that is destined for secretion in VLDL particles (the latent activity).

In summary, we have developed and applied high-throughput LC/MS/MS-based assays to detect the acute metabolic flux of substrates through TG synthesis based on the metabolic conversion of stable isotope-labeled oleic acid or glycerol in hepatic cells and in rodents *in vivo*. In addition, these LC/MS/MS assays provide a means to discern differences between the functions of hepatic DGAT1 and DGAT2. 

REFERENCES

1. Cases, S., S. J. Smith, Y. W. Zheng, H. M. Myers, S. R. Lear, E. Sande, S. Novak, C. Collins, C. B. Welch, A. J. Lusis, et al. 1998. Identification of a gene encoding an acyl CoA:diacylglycerol acyltransferase, a key enzyme in triacylglycerol synthesis. *Proc. Natl. Acad. Sci. USA*. **95**: 13018–13023.
2. Cases, S., S. J. Stone, P. Zhou, E. Yen, B. Tow, K. D. Lardizabal, T. Voelker, and R. W. Farese, Jr. 2001. Cloning of DGAT2, a second mammalian diacylglycerol acyltransferase, and related family members. *J. Biol. Chem.* **276**: 38870–38876.
3. Yen, C., S. J. Stone, S. Koliwad, C. Harris, and R. W. Farese, Jr. 2008. Thematic review series: glycerolipids. DGAT enzymes and triacylglycerol biosynthesis. *J. Lipid Res.* **49**: 2283–2301.
4. Smith, S. J., S. Cases, D. R. Jensen, H. C. Chen, E. Sande, B. Tow, D. A. Sanan, J. Raber, R. H. Eckel, and R. W. Farese, Jr. 2000. Obesity resistance and multiple mechanisms of triglyceride synthesis in mice lacking Dgat. *Nat. Genet.* **25**: 87–90.
5. Stone, S. J., H. M. Myers, S. M. Watkins, B. E. Brown, K. R. Feingold, P. M. Elias, and R. W. Farese, Jr. 2004. Lipopenia and skin barrier abnormalities in DGAT2-deficient mice. *J. Biol. Chem.* **279**: 11767–11776.
6. Yu, X., S. F. Murray, S. K. Pandey, S. L. Booten, D. Bao, X. Song, S. Kelly, S. Chen, R. McKay, B. P. Monia, et al. 2005. Antisense oligonucleotide reduction of DGAT2 expression improves hepatic steatosis and hyperlipidemia in obese mice. *Hepatology*. **42**: 362–371.
7. Choi, C. S., D. B. Savage, A. Kulkarni, X. X. Yu, Z. X. Liu, K. Morino, S. Kim, A. Distefano, V. T. Samuel, S. Neschen, et al. 2007. Suppression of diacylglycerol acyltransferase-2 (DGAT2), but not DGAT1, with antisense oligonucleotides reverses diet-induced hepatic steatosis and insulin resistance. *J. Biol. Chem.* **282**: 22678–22688.
8. Liu, Y., J. S. Millar, D. A. Cromley, M. Graham, R. Croke, J. T. Billheimer, and D. J. Rader. 2008. Knockdown of acyl-CoA:

- diacylglycerol acyltransferase 2 with antisense oligonucleotide reduces VLDL TG and apoB secretion in mice. *Biochim. Biophys. Acta*. **1781**: 97–104.
9. Yamaguchi, K., L. Yang, S. McCall, J. Huang, X. X. Yu, S. K. Pandey, S. Bhanot, B. P. Monia, Y. X. Li, and A. M. Diehl. 2007. Inhibiting triglyceride synthesis improves hepatic steatosis but exacerbates liver damage and fibrosis in obese mice with nonalcoholic steatohepatitis. *Hepatology*. **45**: 1366–1374.
 10. Villanueva, C. J., M. Monetti, M. Shih, P. Zhou, S. M. Watkins, S. Bhanot, and R. V. Farese, Jr. 2009. Specific role for acyl CoA:Diacylglycerol acyltransferase 1 (Dgat1) in hepatic steatosis due to exogenous fatty acids. *Hepatology*. **50**: 434–442.
 11. Qi, J., W. Lang, E. Giardino, G. W. Caldwell, C. Smith, L. K. Minor, A. L. Darrow, G. Willemsens, K. Dewaepeaert, P. Roevens, et al. 2010. High-content assays for evaluating cellular and hepatic diacylglycerol acyltransferase activity. *J. Lipid Res.* **51**: 3559–3567.
 12. Yen, C. L., and R. V. Farese, Jr. 2003. MGAT2, a monoacylglycerol acyltransferase expressed in the small intestine. *J. Biol. Chem.* **278**: 18532–18537.
 13. Ganji, S. H., S. Tavintharan, D. Zhu, Y. Xing, V. S. Kamanna, and M. L. Kashyap. 2004. Niacin noncompetitively inhibits DGAT2 but not DGAT1 activity in HepG2 cells. *J. Lipid Res.* **45**: 1835–1845.
 14. Zhao, G., A. J. Souers, M. Voorbach, H. D. Falls, B. Droz, S. Brodjian, Y. Y. Lau, R. R. Iyengar, J. Gao, A. S. Judd, et al. 2008. Validation of diacylglycerol acyltransferase I as a novel target for the treatment of obesity and dyslipidemia using a potent and selective small molecule inhibitor. *J. Med. Chem.* **51**: 380–383.
 15. Wurie, H. R., L. Buckett, and V. A. Zammit. 2011. Evidence that diacylglycerol acyltransferase 1 (DGAT1) has dual membrane topology in the endoplasmic reticulum of HepG2 cells. *J. Biol. Chem.* **286**: 36238–36247.
 16. McLaren, D. G., T. He, S. P. Wang, V. Mendoza, R. Rosa, K. Gagen, G. Bhat, K. Herath, P. L. Miller, S. Stribling, et al. 2011. The use of stable-isotopically labeled oleic acid to interrogate lipid assembly in vivo: assessing pharmacological effects in preclinical species. *J. Lipid Res.* **52**: 1150–1161.
 17. Patterson, B. W., B. Mittendorfer, N. Elias, R. Satyanarayana, and S. Klein. 2002. Use of stable isotopically labeled tracers to measure very low density lipoprotein-triglyceride turnover. *J. Lipid Res.* **43**: 223–233.
 18. Magkos, F., B. W. Patterson, and B. Mittendorfer. 2007. Reproducibility of stable isotope-labeled tracer measures of VLDL-triglyceride and VLDL-apolipoprotein B-100 kinetics. *J. Lipid Res.* **48**: 1204–1211.
 19. Zammit, V. A., L. K. Buckett, A. V. Turnbull, H. Wure, and A. Proven. 2008. Diacylglycerol acyltransferases: potential roles as pharmacological targets. *Pharmacol Ther.* **118**: 295–302.
 20. Waterman, I. J., and V. A. Zammit. 2002. Differential effects of fenofibrate or simvastatin treatment of rats on hepatic microsomal overt and latent diacylglycerol acyltransferase activities. *Diabetes*. **51**: 1708–1713.
 21. Owen, M. R., C. C. Corstorphine, and V. A. Zammit. 1997. Overt and latent activities of diacylglycerol acyltransferase in rat liver microsomes: possible roles in very-low-density lipoprotein triacylglycerol secretion. *Biochem. J.* **323**: 17–21.